(197)

FEB 5 1968

NATIONAL AERONAUTICS AND SPACE ADMINISTRATION

MSC INTERNAL NOTE NO. 68-FM-17

JANUARY 18, 1968

NAVIGATIONAL CAPABILITIES OF THE SEXTANT AND RANGING DEVICE FOR CSM-ACTIVE RENDEZVOUS

By Jack H. Shreffler,
Mathematical Physics Branch

MISSION PLANNING AND ANALYSIS DIVISION

MANNED SPACECRAFT CENTER
HOUSTON, TEXAS

MSC INTERNAL NOTE NO. 68-FM-17

PROJECT APOLLO

NAVIGATIONAL CAPABILITIES OF THE SEXTANT AND RANGING DEVICE FOR CSM-ACTIVE RENDEZVOUS

By Jack H. Shreffler
Mathematical Physics Branch

January 18, 1968

MISSION PLANNING AND ANALYSIS DIVISION
NATIONAL AERONAUTICS AND SPACE ADMINISTRATION
MANNED SPACECRAFT CENTER
HOUSTON, TEXAS

Approved: James C. McPherson
James C. McPherson, Chief
Mathematical Physics Branch

Approved: John P. Mayer
John P. Mayer, Chief
Mission Planning and Analysis Division

NAVIGATIONAL CAPABILITIES OF THE SEXTANT AND RANGING DEVICE FOR CSM-ACTIVE RENDEZVOUS

By Jack H. Shreffler

SUMMARY

This internal note presents navigation error analysis results which are used to evaluate the navigational capabilities of the sextant, the ranging device, and the two in combination in the interval between CDH and TPI. Specifically, these studies were initiated in response to paragraph 4 of reference 1, which asserts that the sextant's ability to refine relative state uncertainties increases with increasing Δh during the coelliptic phase of a rendezvous sequence. This assertion is basically untrue.

The following conclusions were made from the results of this study.

(a) The sextant's ability to refine relative state uncertainties increases slightly with decreasing Δh during the coelliptic phase.

(b) Disregarding a priori knowledge, the sextant may be used as a navigational instrument to determine relative state uncertainties to within 60 n. mi. and 435 fps (3σ) after 15 minutes of tracking.

(c) The sextant's navigational capability is primarily based on establishing correlations between the in-plane orbital elements which tends to reduce uncertainties upon propagation. Also, the sextant reduces out-of-plane uncertainties extremely well.

(d) Disregarding a priori knowledge, the ranging device and the ranging device with the sextant both have the ability to determine the relative state to within 0.75 n. mi. and 7.5 fps (3σ) after 15 minutes of tracking.

This study considers only circular, coelliptic, earth orbits; the target vehicle is in a 150-n. mi. orbit, and Δh between the vehicles does not exceed 40 n. mi.

INTRODUCTION

The work summarized in this note was initiated to determine the sextant's navigational capability as a function of Δh during the coelliptic phase of a CSM-active rendezvous. It was determined that the sextant's ability to refine the relative state estimate increases slightly with decreasing Δh. This conclusion was diametrically opposed to the currently accepted view, however, so that further examinations of the sextant's capabilities were in order. The additional studies were performed holding the Δh constant at 15 n. mi.

By allowing the intervehicular data to freely correct the relative state estimate, it was determined that the sextant has very little absolute navigational capability. That is, it cannot determine the relative state in the same sense as do the ground radars or rendezvous radar. It is well known, however, that the sextant may be used to produce a reduction of relative state uncertainties. Therefore, a series of runs were made to determine how the sextant may be successfully used. Basically, it was found that the previous knowledge of the state must be heavily relied upon. The sextant merely establishes correlations between the in-plane orbital elements which results in a decrease of uncertainties upon propagation.

With this knowledge, another look was given to the sextant's capability as a function of differential altitude and hopefully, a plausible, albeit qualitative, explanation is given for the new results.

ASSUMPTIONS

The uncertainties associated with both vehicles' states were represented by a covariance matrix generated at CDH + 15 minutes for Apollo 6 (AS-205/101) analyses. Additional uncertainties were introduced from the following sources:

(1) Noise on intervehicular measurements

0.0002 radians for each sextant angle
10 ft in range

(2) Noise on intervehicular measurements

0.0002 radians for each sextant angle
10 ft in range

(3) Uncertainty in μ of the earth:

$\sigma = 1.05 \times 10^{11}\ ft^3/sec^2$

(4) Misalignment of IMU axes:

$\sigma = 5.4 \times 10^{-4}$ radians per axis

(5) Uncertainty in drag acceleration on both vehicles:

$\sigma = 10^{-5}$ ft/sec^2

The target vehicle was assumed to be in a 150-n. mi. circular orbit. First, cases are considered where the Δh between the chaser vehicle and the target was varied. Then, Δh was held constant at 15 n. mi. for all cases considered and, unless otherwise stated, the chaser vehicle was trailing and below. In all cases, 15 intervehicular measurements spaced 1 minute apart are taken. The first mark is assumed to be taken at CDH + 15 minutes. TPI is assumed to be 20 minutes after the last mark.

SEXTANT NAVIGATIONAL CAPABILITY AS A FUNCTION OF Δh

The chaser vehicle was assumed to be in a circular orbit below and behind the target at altitudes of 110, 120, 130, 135, 140, 145, and 148 n. mi. The trailing distance was adjusted so that the angle between the line-of-sight vector and the tangent to the chaser vehicle orbit at the chaser vehicle was equal to 9.2065° at the beginning of tracking for all Δh. The IMU was oriented so that this was also the azimuth angle. The azimuth angle was then computed 10, 15, and 20 minutes later for the various Δh's, as given in the table below.

Δh, n. mi.	Azimuth angles at times after start of tracking, deg		
	10 min	15 min	20 min
40	-28.4253	-46.6925	-64.3696
30	-28.5451	-46.9385	-64.8229
20	-28.6673	-47.1848	-65.2689
15	-28.7298	-47.3092	-65.4911
10	-28.7930	-47.4335	-65.7106
5	-28.8584	-47.5614	-65.9349
2	-28.8996	-47.6412	-66.0738

Two observations may be made concerning these aximuth angles. First, over a 15-minute period the azimuth angles of vehicles along the line of sight will have changed significantly enough to make it possible to determine Δh to about 5 n. mi. Second, the residuals of the azimuth angles at a given time compared to a nominal (e.g., the azimuth angle for Δh = 15 n. mi.) constitute a linear function of Δh. Figure 1 gives a plot of azimuth angle residuals as a function of Δh for a time 15 minutes after azimuth angles were equal for all Δh.

The linearity of the residuals gives the theoretical answer to the question "Does increasing Δh increase the sextant's navigational capability during the coelliptic phase?" The answer is no.

To say that the chaser vehicle has a certain line-of-sight uncertainty means essentially that if a vehicle deviates farther along the line of sight, a residual detectable above noise and bias levels would develop. However, by linearity, the detectable residual will be caused by the same displacement for all Δh. Thus, the same uncertainties may be expected.

The error analysis was performed with a linear error analysis program which treats the simulated sextant measurements in a manner equivalent to the onboard computer. The fit-world covariance was assumed to be reinitialized with a 1000 ft - 1 fps W-matrix before the first mark. Such a small W-matrix means that the estimate of the relative state will be corrected only slightly by the sextant measurements. Instead the a priori knowledge is heavily relied upon. The reason that this is the best procedure is discussed later.

The uncertainties at beginning of tracking and at TPI (assumed to be 20 minutes after the end of tracking) are presented in table I. We see that for greater Δh's the uncertainties increase, which may be explained by the noise and biases on the measurements. At a distance r, noise of angle θ will produce a linear displacement, $r\theta$. Thus, for larger Δh an error in the angle measurement will produce a proportionately larger error in the relative state vector.

ABSOLUTE NAVIGATION CAPABILITY OF THE SEXTANT, RANGING DEVICE, AND BOTH IN COMBINATION

As mentioned previously, using a W-matrix of 1000 ft - 1 fps limits the amount the intervehicular measurements would be allowed to correct the a priori state estimate. In order to determine what navigation capability could be derived almost solely from these measurements, some 15-n. mi. Δh cases were run where the fit-world covariance was reinitialized with a 1 000 000 ft - 1000 fps W-matrix prior to the first mark. Fifteen marks were taken using the sextant, the ranging device, and the two in combination.

The relative state uncertainties are tabulated in table II. It is apparent that the sextant has little navigation capability over short arcs, being able to determine relative state at TPI to within 60 n. mi. and 435 fps (3σ). Almost all the position uncertainty is along the line of sight. It should be noted, however, that the sextant reduces the out-of-plane uncertainties to about 850 ft and 8 fps (3σ).

The addition of the range measurements reduces radically the line-of-sight uncertainty and gives the combination a very definite navigation capability giving 3σ uncertainties at TPI of 0.75 n. mi. and 7.5 fps.

USE OF THE SEXTANT WITH RANGING DEVICE AS OPPOSED TO THE RANGING DEVICE ALONE

It has been indicated in this study as well as some for lunar orbit that, provided out-of-plane uncertainties have been reduced by previous sextant tracking, it is better to use the ranging device alone than to add sextant data. The difference is basically that uncertainties produced from the ranging device only are correlated so that they propagate better. However, some recent studies have shown that the ranging-device alone may provide unstable solutions, giving good results at some points and not at others. This problem needs additional investigation.

Uncertainties resulting from sextant measurements usually decrease upon propagation while those produced by the ranging device, with or without the sextant, increase. However, the use of the ranging device results in such small uncertainties that even upon propagation they are still less than those produced by the sextant alone.

A W-matrix of 1 000 000 ft - 1000 fps was used to reinitialize the fit-world covariance. The optimal variance for processing range measurements is from 500 to 1000 ft when they are taken with sextant marks (ref. 2). When range measurements are taken alone they should be processed with a variance equal to the real noise.

NAVIGATIONAL CAPABILITY OF SEXTANT

It has been shown that if the relative state is determined solely by sextant data and ignoring a priori knowledge, the uncertainties are horrendous. The sextant may be used successfully, however; the sextant's beneficial effects are derived by depending heavily on a priori state knowledge and building correlations between the in-plane orbital elements which cause the uncertainties to decrease upon propagation.

The trajectories considered are the same as for the 15-n. mi. Δh case discussed previously. A W-matrix of 1000 ft - 1 fps was used to reinitialize the fit-world covariance before the first mark.

The sextant has almost no capability to determine line-of-sight range over short arcs; it can, however, refine position uncertainty perpendicular to the line of sight. By using a small W-matrix, the position uncertainties along the line of sight are not allowed to grow and yet some refinement of position uncertainty perpendicular to the line of sight is achieved.

To understand the reason the sextant can produce a reduction of uncertainties, one must look at the relative state covariance matrix. A brief description of the covariance matrix (modified to have correlation coefficients in the lower portion) and the coordinate system is found in the appendix, which should be understood before proceeding with this discussion.

The covariance matrix at the beginning of intervehicular tracking is given in table III. This matrix represents the initial relative state uncertainties for all cases discussed in this note.

Table IV gives relative state covariance matrices for the end of sextant tracking and TPI.

At the end of tracking, there is a strong positive correlation between x and y and a strong negative correlation between x, y, and $\dot{x}$. Looking at the uncertainties in the axes, this may be basically interpreted as saying that, if the chaser vehicle were actually 5800 ft ahead of the nominal, then it would be 1300 ft above and have a radial velocity differing by -7 fps. This correlation in position is along the line of sight, as would be expected.

During a coelliptic phase these correlations have a lasting property. The same strong correlations exist 10 minutes after the end of tracking. However, if a vehicle had a radial velocity differing by -7 fps and was 1300 ft above the nominal, then within 3 minutes it would have the same radius as the nominal and yet still be 5800-ft down range. But this would contradict the strong correlation between x and y. That is, there would be no displacement in x and a large displacement in y.

So, the correlations in the orbital elements combined with their lasting property upon propagation provide a contradiction. The correlations are in some sense opposed to each other. The result might be expected to be a compromise in which a vehicle above and ahead of the nominal (or by the same reasoning below and behind) would move slowly along the line of sight toward the nominal vehicle. The result would be a decrease in uncertainties upon propagation, as is seen in table IV by comparing the RSS uncertainties at end of track and TPI. The uncertainties decrease about 25 percent.

If these kinds of beneficial correlations are produced when the chaser vehicle is below and behind (or above and ahead), what would happen if the chaser vehicle leads and is below the target? To answer this question, a case was run where the chaser vehicle was leading through the tracking period. The Δh was again 15 n. mi. The initial elevation angle of the target was arranged so that the elevation angle at the 15th mark was equal to the elevation angle at the first mark in the previous case. The resulting covariance matrices are given in table V.

At the end of track, x and $\dot{x}$ are positively correlated, and x and y are negatively correlated. By the same reasoning as in the previous discussion, a vehicle ahead and below of its nominal position would tend to move out along its line of sight, thus increasing uncertainties upon propagation.

Indeed, comparison of end-of-track uncertainties and TPI uncertainties show this effect. The uncertainties increase about 20 percent.

This result indicates that the sextant should not be used alone if the chaser vehicle is either below and ahead or above and behind the targ[illegible]. This conclusion applies only during coelliptic situations. Fort[illegible]ately, this type of tracking is not planned for any mission.

The sextant is useful as a navigation instrument in two respects. First, it reduces out-of-plane uncertainties very effectively. This is especially important in lunar orbit. Secondly, if the chaser vehicle is below and behind or above and ahead of the target, sextant marks will produce correlations that will cause uncertainties to propagate downward.

The beneficial correlations seem to last beyond the end of sextant tracking only when in a coelliptic situation. Reference 3 gives results of error analysis of a rendezvous sequence for AS-205/101. Despite 35 sextant sightings taken between NCC and CDH, not a coelliptic sequence, no reduction of uncertainties was achieved. With only 15 marks between NSR and TPI, a 70 percent reduction was effected.

ANOTHER LOOK AT SEXTANT EFFICIENCY AS A FUNCTION OF Δh

As previously noted, uncertainties at TPI decreased with decreasing Δh. Actually the uncertainties at the end of tracking differ only slightly, however. The difference is produced by propagational effects.

In table VI the covariance matrices after the 15 sextant marks have been incorporated (actually epoched to the beginning of the tracking arc) for Δh = 40 n. mi. and Δh = 10 n. mi. Note the absence of strong correlations in the former and the existence of strong correlations in the latter. By the previous analysis, this is the cause of the different propagation properties.

For the Δh = 40 n. mi. case, there is more difficulty building a strong correlation between x and y since the uncertainties perpendicular to the line of sight are more difficult to remove due to noise and bias on the angle measurements. That is, at a distance r, noise of angle θ will produce a linear displacement, $r\theta$, perpendicular to the line of sight.

CONCLUSIONS

(1) The sextant's ability to reduce relative state uncertainties is based almost solely on establishing correlations between in-plane orbital elements which tend to reduce uncertainties upon propagation. Also the sextant reduces out-of-plane uncertainties extremely well.

(2) The beneficial correlations produced by sextant sightings must have a lasting property to effectively reduce uncertainties. The correlations seem to endure after the last sextant mark only when a coelliptic phase is being considered. Under other conditions, the correlations disappear rapidly and the benefits derived from sextant tracking are doubtful.

(3) The sextant's ability to reduce relative state uncertainties increases slightly with decreasing Δh, during the coelliptic phase. At smaller Δh, the sextant is able to produce stronger correlations.

(4) The ranging device and ranging device with sextant both have a definite navigation capability. That is, they produce a reduction of uncertainties by solving a dynamic problem and not just building beneficial correlations and depending on propagational effects.

TABLE I - 3σ POSITION AND VELOCITY UNCERTAINTIES BEFORE SEXTANT TRACKING AND AT TPI FOR VARIOUS Δh

Δh, n. mi.	3σ uncertainties at CDH + 15 min		3σ uncertainties at TPI	
	Position, ft	Velocity, fps	Position, ft	Velocity, fps
2	21 000	30.3	8700	9.5
5	21 000	30.3	9300	10.6
10	21 000	30.3	10 500	13.1
15	21 000	30.3	12 150	16.4
20	21 000	30.3	14 250	20.4
30	21 000	30.3	19 400	29.5
40	21 000	30.3	25 200	39.3

TABLE II - RELATIVE POSITION AND VELOCITY UNCERTAINTIES

FOR Δh = 15 N. MI.

[1 000 000 ft - 1000 fps W-matrix used to reinitialize the fit-world covariance at the beginning of intervehicular tracking]

Data type	3σ uncertainties at CDH + 15 min (beginning of track)		3σ uncertainties at CDH + 30 min (end of track)		3σ uncertainties at TPI	
	Position, ft	Velocity, fps	Position, ft	Velocity, fps	Position, ft	Velocity, fps
Sextant only	21 000	30.3	727 900	830	392 000	435
Ranging device only	21 200	30.3	1560	1.8	3080	4.1
Sextant with ranging device	21 200	30.3	1330	2.34	5030	7.9

TABLE III.- MODIFIED RELATIVE STATE COVARIANCE MATRIX REPRESENTING

INITIAL UNCERTAINTIES FOR CASES CONSIDERED IN THIS REPORT

.115526+08	.170117+08	-.189204+05	-.237500+05	-.181561+05	.180422+02
.807173-00	.384487+08	-.333810+05	-.528386+05	-.296198+05	.318216+02
-.329062-01	-.318233-01	.286171+05	.465177+02	.310670+02	.963523+01
-.818239-00	-.997855-00	.322004-01	.729267+02	.413000+02	-.443198-01
-.988263-00	-.883753-00	.339763-01	.894737-00	.202161+02	-.296135-01
.219096-01	.211818-01	.235089-00	-.214209-01	-.226132-01	.586995-01

SQRT((1,1)+(2,2)+(3,3)) = .707318+04 SQRT((4,4)+(5,5)+(6,6)) = .101095+02

SQRT(1, 1) =	.339891+04
SQRT(2, 2) =	.620070+04
SQRT(3, 3) =	.169166+03
SQRT(4, 4) =	.853971+01
SQRT(5, 5) =	.540519+01
SQRT(6, 6) =	.242280-00

TABLE IV.- MODIFIED RELATIVE STATE COVARIANCE MATRICES REPRESENTING UNCERTAINTIES

WHEN Δh = 15 N. MI. AND THE CHASER VEHICLE TRAILS THE TARGET VEHICLE

(a) Uncertainties after 15 sextant marks

.1733326+07	.7572823+07	-.2561470+03	-.9047006+04	-.4654826+03	-.1956982+01
.9838027+00	.3418371+08	-.1147666+04	-.4075155+05	-.2066946+04	-.8768213+01
-.8582023-03	-.8658581-03	.5139477+05	.1379763+01	.6397882-01	-.1704998+02
-.9843572+00	-.9984414+00	.8718331-03	.4873308+02	.2521952+01	.1054121-01
-.8232263+00	-.8231432+00	.6571018-03	.8411644+00	.1844540+00	.4882090-03
-.4413814-02	-.4453165-02	-.2233221+00	.4483799-02	.3375429-02	.1134136+00

SQRT((1,1)+(2,2)+(3,3)) = .5997369+04 SQRT((4,4)+(5,5)+(6,6)) = .7002211+01

SQRT(1, 1)	=	.1316558+04
SQRT(2, 2)	=	.5846684+04
SQRT(3, 3)	=	.2267041+03
SQRT(4, 4)	=	.6980908+01
SQRT(5, 5)	=	.4294811+00
SQRT(6, 6)	=	.3367694+00

(b) Uncertainties at TPI

.1030047+07	.2211160+07	-.1236345+04	-.2649268+04	-.4974395+03	-.3709770-01
.5254093+00	.1686693+08	-.8749682+04	-.2321661+05	.1917962+03	-.2255827+00
-.4341730-02	-.7666581-02	.7722266+05	.1203404+02	-.1095301+00	.2214615+00
-.4557053+00	-.9964220+00	.7653116-02	.3218658+02	-.5487626+00	.3035946-00
-.7804398+00	.7508022-01	-.6336727-03	-.1555072+00	.3868948+00	-.1150251+00
-.1295540-03	-.1965604-03	.2851901+00	.1914983-03	-.6617665-04	.7808779-01

SQRT((1,1)+(2,2)+(3,3)) = .4241958+04 SQRT((4,4)+(5,5)+(6,6)) = .5714155+01

SQRT(1, 1)	=	.1024718+04
SQRT(2, 2)	=	.4106937+04
SQRT(3, 3)	=	.2778896+03
SQRT(4, 4)	=	.5673322+01
SQRT(5, 5)	=	.6220087+00
SQRT(6, 6)	=	.2794419+00

TABLE V.- MODIFIED RELATIVE STATE COVARIANCE MATRICES REPRESENTING

UNCERTAINTIES WHEN Δh = 15 N. MI. AND THE CHASER VEHICLE LEADS THE TARGET VEHICLE

(a) Uncertainties after 15 sextant marks

.1765195+07	-.9834586+07	.3248054+03	.1156506+05	.3907632+03	.2004828+01
-.9715561+00	.5804750+08	-.1918308+04	-.6786412+05	-.2652883+04	-.1184056+02
.8247356-03	-.8494045-03	.8786670+05	.2247323+01	.1612053+00	.7035696+01
.9766395+00	-.9993812+00	.8506209-03	.7943913+02	.3139059+01	.1387137-01
.3945967+00	-.4671566+00	.7296313-03	.4725181+00	.5555556+00	.9953688-03
.5957449-02	-.6135645-02	.9370753-01	.6144432-02	.5272296-02	.6415652-01

SQRT((1,1)+(2,2)+(3,3)) = .7739546+04　　SQRT((4,4)+(5,5)+(5,6)) = .8947561+01

SQRT(1, 1) =	.1328606+04
SQRT(2, 2) =	.7618891+04
SQRT(3, 3) =	.2964231+03
SQRT(4, 4) =	.8912863+01
SQRT(5, 5) =	.7453560+00
SQRT(6, 6) =	.2532913+00

(b) Uncertainties at TPI

.3086939+07	-.1457760+08	.3541526+04	.1833439+05	.6530143+03	.9318703+00
-.9319573+00	.7925960+08	-.1770165+05	-.9772559+05	-.4013559+04	-.4621479+01
.8666805-02	-.8549101-02	.5409221+05	.2223628+02	.1766002+01	-.1956663+02
.9489412+00	-.9982038+00	.8694241-02	.1209278+03	.5008842+01	.5816933-02
.3898570+00	-.4728794+00	.7964722-02	.4777722+00	.9088800+00	.4904608-03
.1596174-02	-.1562226-02	-.2531848+00	.1591914-02	.1548246-02	.1104134+00

SQRT((1,1)+(2,2)+(3,3)) = .9077480+04　　SQRT((4,4)+(5,5)+(6,6)) = .1104297+02

SQRT(1, 1) =	.1756968+04
SQRT(2, 2) =	.8902786+04
SQRT(3, 3) =	.2325773+03
SQRT(4, 4) =	.1099672+02
SQRT(5, 5) =	.9533519+00
SQRT(6, 6) =	.3322852+00

TABLE VI.- MODIFIED RELATIVE STATE COVARIANCE MATRICES

REPRESENTING UNCERTAINTIES AFTER 15 SEXTANT MARKS

(a) Δh = 40 n. mi.

.1720445+07	.8217285+07	-.9209963+03	-.8532096+04	.3869516+03	.5342638+01
.7920960+00	.6255471+08	-.6883881+04	-.6185997+05	.5526400+04	.3993387+02
-.8273030-03	-.1149443-02	.5733653+06	.6681971+01	-.6675415+00	-.2917959+02
-.8269389+00	-.9943009+00	.1121829-02	.6187620+02	-.5330593+01	-.3876181-01
.2994897+00	.7093459+00	-.8949697-03	-.6879542+00	.9703053+00	.3871750-02
.6447882-02	.7992693-02	-.6100217-01	-.7800529-02	.6222071-02	.3990583+00

SQRT((1,1)+(2,2)+(3,3)) = .8052858+04 SQRT((4,4)+(5,5)+(6,6)) = .7952708+01

SQRT(1, 1) =	.1311657+04
SQRT(2, 2) =	.7909153+04
SQRT(3, 3) =	.7572089+03
SQRT(4, 4) =	.7866143+01
SQRT(5, 5) =	.9850407+00
SQRT(6, 6) =	.6317106+00

(b) Δh = 10 n. mi.

.1548056+07	.8929289+07	-.2500247+03	-.1017405+05	-.2681411+03	.1500083+01
.9863186+00	.5294347+08	-.1482085+04	-.6015079+05	-.1446458+04	.8892140+01
-.1040697-02	-.1054877-02	.3728464+05	.1678906+01	.2912047-01	-.3252698+01
-.9888057+00	-.9996439+00	.1051409-02	.6838796+02	.1645337+01	-.1007301-01
-.6469095+00	-.5967237+00	.4526963-03	.5972258+00	.1109820+00	-.1747280-03
.7380605-02	.7481181-02	-.1031214+00	-.7456578-02	-.3210748-02	.2668454-01

SQRT((1,1)+(2,2)+(3,3)) = .7384363+04 SQRT((4,4)+(5,5)+(6,6)) = .8278021+01

SQRT(1, 1) =	.1244209+04
SQRT(2, 2) =	.7276226+04
SQRT(3, 3) =	.1930923+03
SQRT(4, 4) =	.8269701+01
SQRT(5, 5) =	.3331397+00
SQRT(6, 6) =	.1633540+00

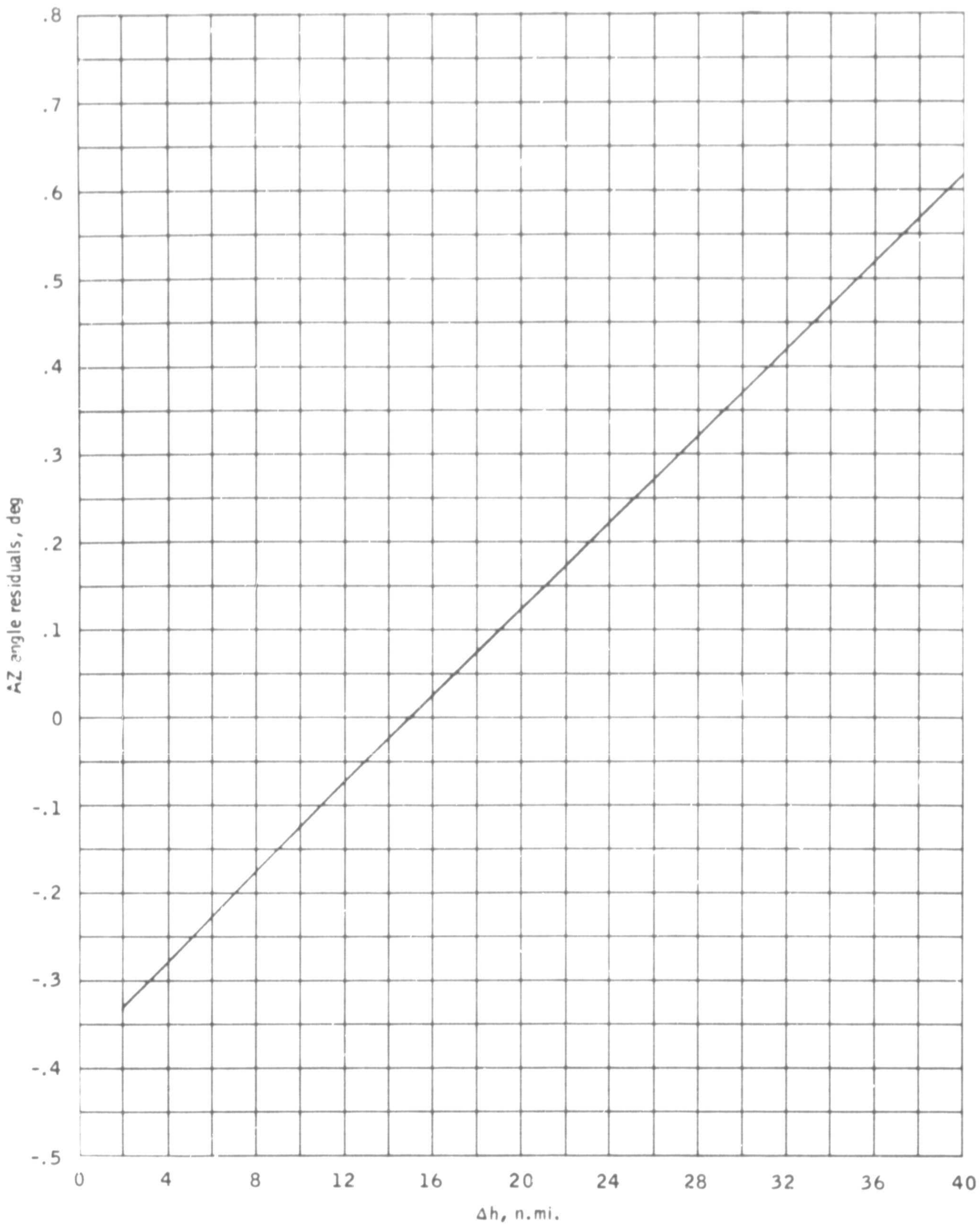

Figure 1.- Azimuth angle residuals as a function of Δh.

APPENDIX A

DEFINITION OF LOCAL COORDINATE SYSTEM AND MODIFIED RELATIVE STATE COVARIANCE MATRIX

APPENDIX A- DEFINITION OF LOCAL COORDINATE SYSTEM AND MODIFIED RELATIVE STATE COVARIANCE MATRIX

LOCAL COORIDNATE SYSTEM

The local coordinate system used in this report is defined as follows: z is measured in the direction of the angular momentum vector, x is measured radially, and y completes the right-hand system.

MODIFIED RELATIVE STATE COVARIANCE MATRIX IN LOCAL COORDINATE SYSTEM

The form of the modified relative state covariance matrices presented in this report is given below.

$$
\begin{array}{cccccc}
\sigma_{xx} & \sigma_{xy} & \sigma_{xz} & \sigma_{x\dot{x}} & \sigma_{x\dot{y}} & \sigma_{x\dot{z}} \\
\rho_{yx} & \sigma_{yy} & \sigma_{yz} & \sigma_{y\dot{x}} & \sigma_{y\dot{y}} & \sigma_{y\dot{z}} \\
\rho_{zx} & \rho_{zy} & \sigma_{zz} & \sigma_{z\dot{x}} & \sigma_{z\dot{y}} & \sigma_{z\dot{z}} \\
\rho_{\dot{x}x} & \rho_{\dot{x}y} & \rho_{\dot{x}z} & \sigma_{\dot{x}\dot{x}} & \sigma_{\dot{x}\dot{y}} & \sigma_{\dot{x}\dot{z}} \\
\rho_{\dot{y}x} & \rho_{\dot{y}y} & \rho_{\dot{y}z} & \rho_{\dot{y}\dot{x}} & \sigma_{\dot{y}\dot{y}} & \sigma_{\dot{y}\dot{z}} \\
\rho_{\dot{z}x} & \rho_{\dot{z}y} & \rho_{\dot{z}z} & \rho_{\dot{z}\dot{x}} & \rho_{\dot{z}\dot{y}} & \sigma_{\dot{z}\dot{z}}
\end{array}
$$

1σ RSS position uncertainty $\qquad$ 1σ RSS velocity uncertainty

1σ uncertainty in x

1σ uncertainty in y

1σ uncertainty in z

1σ uncertainty in $\dot{x}$

1σ uncertainty in $\dot{y}$

1σ uncertainty in $\dot{z}$

Correlation coefficients, ρ_{ij}, appear in the lower left half of the matrix and are given by

$$\rho_{ij} = \frac{\sigma_{ij}}{\sqrt{\sigma_{ii}}\,\sqrt{\sigma_{jj}}}$$

Table A-I is a typical relative state covariance matrix measured in the local coordinate system of the chaser vehicle. Actually, in practice the covariance matrices differ little from one vehicle's system to another since they are so close during rendezvous.

Correlation coefficients appear in the lower left half of the matrix. Correlations are called "strong" or "significant" if they exceed 0.9 in absolute value. We notice in this example that there is a strong positive correlation between x and y and a strong negative correlation between x and $\dot{x}$. By reading the square roots of the diagonal elements we get the uncertainties in each component, but the correlations give more information. For this covariance we know that if a vehicle is ahead of the nominal (positive y) then it is higher (positive x) and has a greater velocity downward (negative $\dot{x}$). Another covariance with the same diagonal terms may represent a much different type of uncertainty because of different correlations.

TABLE A-I.- TYPICAL MODIFIED RELATIVE STATE COVARIANCE MATRIX

MEASURED IN LOCAL COORDINATE SYSTEM OF CHASER VEHICLE

.392439+06	.431763+07	-.133796+03	-.503062+04	-.336028+03	.689362-00
.963583-00	.511612+08	-.156631+04	-.594041+05	-.373012+04	.807065+01
-.910310-03	-.933340-03	.550469+05	.182311+01	.124293+00	-.129610+01
-.966718-00	-.999794-00	.935431-03	.690036+02	.433504+01	-.939378-02
-.957155-00	-.930562-00	.945308-03	.931216-00	.314061-00	-.640397-03
.538495-02	.552152-02	-.270329-01	-.553382-02	-.559194-02	.417599-01

SQRT((1,1)+(2,2)+(3,3)) = .718392+04   SQRT((4,4)+(5,5)+(6,6)) = .832823+01

SQRT(1, 1) =	.626450+03
SQRT(2, 2) =	.715271+04
SQRT(3, 3) =	.234621+03
SQRT(4, 4) =	.830684+01
SQRT(5, 5) =	.560412-00
SQRT(6, 6) =	.204352-00

REFERENCES

1. Pixley, Paul T.: Earth Orbit CSM Active Rendezvous Capability. MSC Memorandum 67-FM46-217, October 20, 1967.

2. Shreffler, J.: Onboard Navigation. MSC Memorandum 67-FM46-197, September 25, 1967.

3. Shreffler, J.: Navigation Error Analyses of the First Rendezvous Sequence of AS-205/101. MSC Internal Note 67-FM-185, November 30, 1967.